Structural Studies on Alkylisocyanate Polymers by Thermal Degradation Tandem Mass Spectrometry

Tapan K. Majumdar, Marcos N. Eberlin,* and R. Graham Cooks
Department of Chemistry, Purdue University, West Lafayette, Indiana, USA

Mark M. Green, Beth Muñoz, and Mike P. Reidy
Department of Chemistry, Polytechnic University, Brooklyn, New York, USA

Homopolymers and copolymers of alkylisocyanates having n-hexyl, 2,6-dimethylheptyl, 3,7-dimethyloctyl, and (2,2-dimethyl-1,3-dioxolan-4-yl)methyl substituents underwent thermal degradation in the course of desorption electron ionization to yield trimers and monomers that were characterized in situ by tandem mass spectrometry. The trimers were trisubstituted cyanuric acids, the protonated molecules displaying a characteristic series of alkene eliminations on collision-induced dissociation to yield protonated cyanuric acid, m/z 130. Confirmation of the identity of the pyrolysates was obtained by using two types of MS^3 experiments: the reaction intermediate scan and the two-dimensional familial scan. The ion chemistry of the trimers and of the protonated monomer, the alkylisocyanate, was elucidated. Among the many interesting fragmentation processes undergone by the ionized trimers were α and β C—C bond cleavages and charge-remote fragmentations, which provided information on branching in the alkyl substituent. The dioxolane-containing substituent showed unique ion chemistry. The monomer distribution in the copolymers was deduced from the abundances of the various protonated trimers. The distribution was found to be random in all copolymers except that containing the dioxolane substituent. (J Am Soc Mass Spectrom 1991, 2, 130–148)

Polyisocyanates [1], also known as N-substituted 1-nylons, are linear high molecular weight polymers [2, 3] having liquid-crystalline properties [4]. In this study we investigate the application of tandem mass spectrometry (MS/MS) to these liquid crystal polymers. This is appropriate because mass spectrometry has been shown to be useful in examining the polyisocyanates [5] and, in general, is seeing gradually increasing use as a tool for polymer characterization [6–8] as a result of the lifting of the principal limitations of the technique through advances in ionization methods [9–11] and extensions in mass range [12–15]. The present study has three major objectives: (1) to investigate the usefulness of pyrolysis/MS/MS in identifying the products of thermal degradation of polyisocyanates, (2) to investigate the ion chemistry of the polyisocyanate pyrolysates, and (3) to establish whether mass spectrometric methods are useful in determining the distribution of monomers in copolymers.

Pyrolysis, when coupled with spectroscopic techniques, is a generally useful approach to the analysis of polymers and other complex nonvolatile organic materials. Since the introduction of pyrolysis/mass spectrometry by Zemany [16], it has been applied extensively in polymer analysis. Commonly, gas chromatography combined with mass spectrometry is used to characterize pyrolysates [17–19] although the method has obvious limitations. In other experiments, pyrolysis of nonvolatile samples is followed by immediate ionization of the pyrolysate and mass analysis of the resulting gas-phase ions [6–8, 16–22]. Three methods are commonly used in pyrolysis/mass spectrometry: (1) Curie-point pyrolysis [23], which involves rapid inductive heating (10^2–10^4 K/s), (2) pyrolysis by means of laser irradiation [24], and (3) pyrolysis induced by slower resistive heating of a sample in a direct insertion probe or furnace pyrolyzer [25]. Two versions of the last method, desorption chemical ionization (DCI) and desorption electron ionization (DEI) [26], utilize relatively rapid heating of a sample placed on a thin wire that is introduced directly into the ionization chamber of an electron impact or chemical ionization source. This procedure,

*On leave from Universidade Estadual de Campinas, C.P. 6154, 13081, Campinas, SP, Brazil.
Address reprint requests to R. Graham Cooks, Department of Chemistry, Purdue University, West Lafayette, IN 47907.

like the closely related particle impact desorption methods of ionization [27], can result in vaporization of thermally labile molecules without thermal degradation. For example, laser desorption Fourier-transform mass spectrometry has been applied successfully to determine the molecular weight distributions and copolymer compositions of a series of methylmethacrylate/butylacrylate, methylmethacrylate/styrene, and poly(ethylene glycol)/poly(propylene glycol) copolymers [28].

Tandem mass spectrometry provides enhanced capabilities for elucidating molecular structures, especially for compounds present in mixtures [29, 30]. The combination of desorption ionization methods with MS/MS has proven of value in biopolymer research, especially peptide sequencing [31, 32], and MS/MS may also have much to offer in structural characterization of other types of polymers. This is indicated by the studies of Lattimer et al. [6], who used MS/MS combined with fast atom bombardment to study polyglycols and found the technique useful for direct analysis of the structures of individual components in mixtures of oligomers. Similarly, Montaudo and coworkers [20, 21] used MS/MS in structural studies of mixtures of pyrolysis products of polyamides.

An extension of the MS/MS concept is embodied in MS^3 experiments, which employ three stages of mass analysis [33]. Two types of MS^3 experiments are employed in this study and are implemented by using a pentaquadrupole mass spectrometer [34]. In the first type, the reaction intermediate scan, intermediate ions connecting a specific parent ion and a terminal fragment ion are recorded [35]. In the second type, the familial scan, the parents and daughters of a particular mass-selected ion are recorded in the form of a two-dimensional mass spectrum [35]. These are new capabilities in mass spectrometry and it is clearly of interest to establish their utility.

Experimental

Mass spectra and MS/MS experiments were recorded by using a Finnigan TSQ 4500 mass spectrometer. Solid samples were placed on a rhenium wire filament of a direct exposure probe or in a glass vial in a direct insertion probe for introduction into the ion source of the mass spectrometer. Typical sample sizes were approximately 1 μg for DEI and DCI mass spectra and 10 μg for MS/MS experiments. The ion source temperature was 190 °C and background pressure in the ion source was 3×10^{-8} torr. Pyrolysis of the polymers was carried out within the ion source of the mass spectrometer by heating the probe from 20 °C to 400 °C at a rate of 100 °C/s. The instrument was scanned during the entire temperature ramp. Pyrolysates appeared within the temperature range 200–400 °C. The source pressure during DEI was approximately 2×10^{-7} torr. The pyrolysates were

ionized either by 15-eV or 70-eV DEI or by DCI by using reagent ions generated from ammonia, isobutane, or methane reagent gases. The chemical ionization (CI) gas pressure in the ion source was 0.5 torr. The quadrupole mass analyzer was scanned from 100 u to 600 u at a rate of 1000 u/s during the collection of DEI and DCI mass spectra. Fragmentation of the ionized pyrolysates was investigated with MS/MS by using DCI for the production of protonated and other adduct ions and DEI for the formation of radical cations. Parent ions, mass-selected by using the first quadrupole (Q1), were collided with argon collision gas at 20 eV and a pressure of 2.0 mtorr (multiple collision conditions) in the second quadrupole (Q2) to generate daughter spectra, which were recorded by scanning the third quadrupole (Q3). Parent spectra were recorded under the same conditions.

Reaction intermediate and familial scans were recorded by using a custom-built pentaquadrupole instrument [35]. About 0.5 mg of the solid sample was introduced via a direct insertion probe, which was heated from an initial temperature of 35 °C to the final temperature of 180 °C at a rate of 120 °C/min during pyrolysis. The spectra were acquired at the final temperature. The background pressure in the ion source was 2×10^{-7} torr and the maximum indicated sample pressure during pyrolysis was 6×10^{-5} torr. The pyrolysates were ionized by 25-eV electron impact. For the reaction intermediate scans, the parent ions were mass-selected by Q1, and the fifth quadrupole (Q5) was set to select a specific fragment ion of interest while scanning Q3. For the familial scan, Q3 was set at a particular mass-to-charge ratio value while scanning both Q1 and Q5 to produce a two-dimensional output. Argon was used as collision gas in both regions at nominal pressures 1×10^{-5} torr and 3×10^{-5} torr (as measured by remote ion gauges) for the second (Q2) and fourth (Q4) quadrupoles, respectively. The quadrupoles were operated at offset voltages, relative to the grounded ion source, of Q1 = −10 V, Q2 = −4 V, Q3 = −5 V, Q4 = −8 V, and Q5 = −5 V. The MS^3 spectra were recorded by scanning the quadrupoles at a rate of 2 u/s using a custom-built MS^3 data system that employed a Keithley Series 500 measurement and control system, a Zenith Z-200 PC, and software written in the "C" language [35].

Copolymers were synthesized from mixtures containing two monomers in various mole ratios: Polymer-IV was synthesized from n-hexylisocyanate and 2,6-dimethylheptylisocyanate in the mole ratio 63:37, Polymer-V from a 50:50 mole ratio of 2,6-dimethylheptylisocyanate and its homologue 3,7-dimethyloctylisocyanate, and Polymer-VI from n-hexylisocyanate and (2,2-dimethyl-1,3-dioxolan-4-yl)methylisocyanate in the mole ratio 88:12 [36, 37]. The various polyisocyanates were synthesized by following detailed procedures discussed in the Ph.D. theses of M. P. Reidy

Table 1. Direct pyrolysis mass spectra of Polymer-I, obtained with different ionization methods[a]

	DEI methods		DCI methods		
m/z	70 eV	15 eV	NH$_3$	i-butane	CH$_4$
399	—	—	36	—	—
382	5	17	100	100	100
381	1	4	—	—	—
366	—	—	—	—	4
352	3	3	—	—	1
338	1	2	—	—	1
324	2	3	—	—	—
311	3	3	—	—	—
298	100	100	—	—	—
281	3	6	—	—	—
256	2	1	—	—	—
242	3	2	—	—	—
228	5	1	—	—	—
214	5	—	—	15	—
158	1	—	—	—	—
144	2	—	—	—	—
130	7	—	—	—	—
128	1	—	—	2	44
112	2	2	—	—	—

[a]Isotopic peaks and ions less than 1% in relative abundance are not reported.

and B. Muñoz (Polytechnic University, 1990). The synthesis of poly(2,6-dimethylheptylisocyanate) and poly(2,2-dimethyl-1,3-dioxolan-4-yl)methylisocyanate and their copolymers with n-hexylisocyanate has appeared in the literature [36, 37].

Results and Discussion

Homopolymers – Major Pyrolysis Products and Fragmentation Pathways

The pyrolysis mass spectra of poly(n-hexyl)isocyanate (Polymer-I) display m/z 382 as the highest mass ion under DEI conditions and as the most abundant ion under DCI (Table 1), which suggests that this ion represents an ionized form of the predominant pyrolysis product. The daughter spectrum of ion m/z 382 shows major fragments at m/z 298, 214, and 130 (Table 2), ions which appear to arise from m/z 382 by sequential loss of molecules of hexene (C$_6$H$_{12}$, 84 u). This reaction sequence is clearly revealed in the reaction intermediate spectrum [35] (Figure 1), which shows only the ions m/z 298 and 214 as intermediates of significant abundance connecting ion m/z 382 with the fragment m/z 130. The two-dimensional familial scan, acquired by selecting ion m/z 130 as the intermediate, also confirms this fragmentation pathway, as well as allowing structural assignments for these ions. This spectrum (Figure 2) shows parent ions, m/z 382, 298, and 214, corresponding to the successive losses of hexene units. Since each of the parent ions generates the same set of daughter ions, m/z 87, 70, and 44, when they fragment via m/z 130 to lower-mass ions, it is clear that each parent produces an identical product m/z 130. The set of fragments displayed by ion m/z 130 suggests it to be

protonated cyanuric acid, and it is therefore concluded that the individual parent ions are n-hexylated forms of this ion.

In order to confirm the structure of ion m/z 130, a daughter spectrum of protonated cyanuric acid was recorded by using an authentic sample of this compound. The similarity of this spectrum with the daughter spectrum of m/z 130 generated by pyrolysis of Polymer-I (Figure 3) confirms that they indeed have the same structure. The fragmentation pathway proposed for this ion is shown in Scheme I.

From the above information one can conclude that the principal pyrolysis product of Polymer-I is the neutral trimer which, upon DCI and DEI, yields the protonated trimer [M + H]$^+$ at m/z 382 and, under DEI conditions, a minor amount of the radical cation of the trimer, M$^{+ \cdot}$ at m/z 381. The use of ammonia as reagent gas leads, in addition to [M + H]$^+$, to an [M + NH$_4$]$^+$ adduct at m/z 399. Formation of the protonated trimer in greater abundance than the molecular ion during DEI is due to self-protonation, which is probably a result of the high local pressure of the pyrolysate in the ion source.

The protonated and the radical cation forms of the molecular ion of the n-hexylisocyanate trimer fragment principally by a convergent route (Scheme I) that involves loss of their n-hexyl groups (R$_1$). The proposed mechanism for loss of the stable hexenyl radical from the trimer radical cation, a process that must involve transfer of two hydrogens from the leaving alkyl group, is also shown in Scheme I.

Confirmation of these assignments, as well as further detail of the ion chemistry of the pyrolysate, is available by examination of the daughter and parent ion spectra of the major fragment ions. The hexene elimination process is clearly seen in the daughter

Table 2. MS/MS spectra of the major ions of Polymer-I[a]

Selected ion m/z	Daughter ions m/z (% relative abundance)	Parent ions m/z (% relative abundance)
399[b]	382(100), 298(84), 214(45), 130(13)	None observed
382	298(15), 214(40), 130(100), 128(16), 85(31), 59(1), 57(6), 43(11)	399(100)[b]
381[c]	298(100), 256(3), 242(3), 228(3), 214(62), 144(5), 130(88), 128(3), 85(5), 70(4), 43(3)	None observed
311[c]	282(5), 266(18), 255(14), 241(14), 228(62), 158(28), 144(100), 113(18), 87(5), 85(53), 70(6), 59(11), 57(37), 43(24)	381(100), 353(5)
298[c]	256(1), 214(25), 144(1), 130(100), 128(1), 87(8), 85(8), 70(1), 59(2), 57(7), 43(12)	382(100)
256[d]	214(7), 179(2), 172(33), 144(1), 130(100), 128(3), 93(3), 87(17), 85(8), 70(2), 59(3), 57(5), 43(32)	382(100)
228[d]	144(100), 128(1), 101(5), 87(10), 85(3), 70(2), 59(2), 57(45), 44(12), 43(45)	382(100), 366(18), 352(34), 311(97)
214[d]	130(45), 87(30), 85(8), 70(8), 59(3), 57(15), 44(30), 43(100), 41(2)	382(100), 352(3), 298(23)
184	142(1), 128(6), 85(34), 57(100), 43(65), 41(10), 29(4), 27(3)	None observed
158[d]	130(18), 87(14), 72(1), 70(7), 59(100), 57(1), 44(62), 43(5), 42(5)	382(70), 352(4), 311(21), 298(40), 242(100), 212(26)
144[d]	87(15), 70(12), 59(3), 58(94), 57(6), 44(100)	382(50), 352(30), 312(13), 311(24), 228(100)
130[d]	87(20), 70(18), 44(100)	382(15), 366(1), 352(2), 298(100), 256(1), 242(1), 214(5), 184(1)
128	127(3), 112(5), 98(2), 85(5), 84(10), 70(21), 59(7), 57(34), 43(100)	382(100), 298(8), 242(1)

[a]Conditions: Isobutane DCI (unless otherwise noted), 20-eV collisions on Argon (2 mtorr).
[b]Ammonia DCI is used.
[c]15-eV DEI is used.
[d]70-eV DEI is used.

spectra of ions m/z 298 and 214 (Table 2). The parent spectra of all the major ions show the protonated trimer, m/z 382, as their highest-mass precursor, and their daughter spectra yield either m/z 144 or m/z 130.

The formation of the cyclic trimer is also observed in the direct pyrolysis mass spectra of *poly(2,6-dimethylheptyl)isocyanate* (Polymer-II) as $[M + H]^+$ (m/z 508), $M^{+\cdot}$ (m/z 507), and in the case of NH_3 DCI, $[M + NH_4]^+$ (m/z 525) (Table S-1). The fragmentation of ion m/z 508 by sequential eliminations of the

2,6-dimethylheptyl groups (R_2) as nonene (126 u) is responsible for the abundant ions at m/z 382, 256, and 130 in the mass spectrum. This fragmentation sequence, familiar from Scheme I, is also evident in its daughter spectrum. The reaction intermediate spectrum (not reproduced since it matches that discussed below for Polymer-IV) clearly shows that the fragment ions m/z 382 and 256 are the intermediates that connect the ions m/z 508 and 130. The isobaric
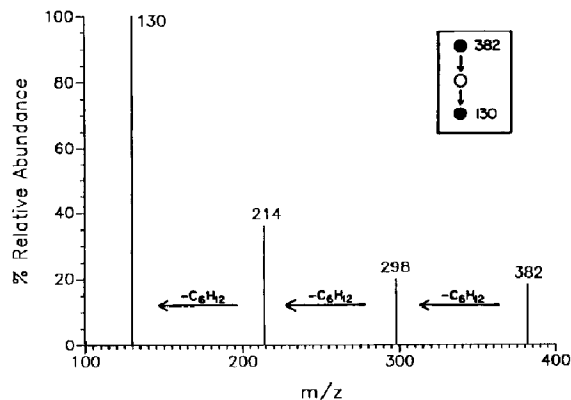

Figure 1. MS[3] reaction intermediate spectrum of the protonated trimer from Polymer-I.
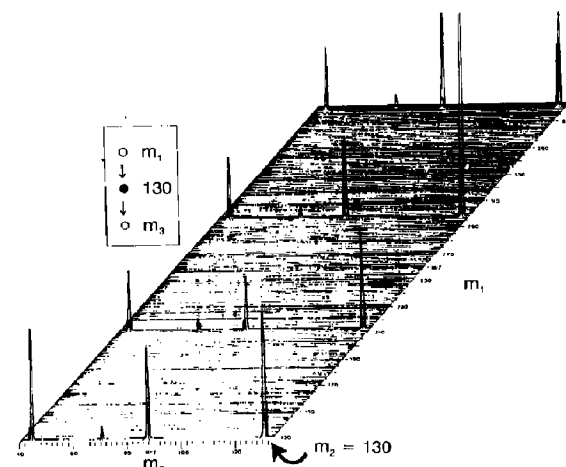

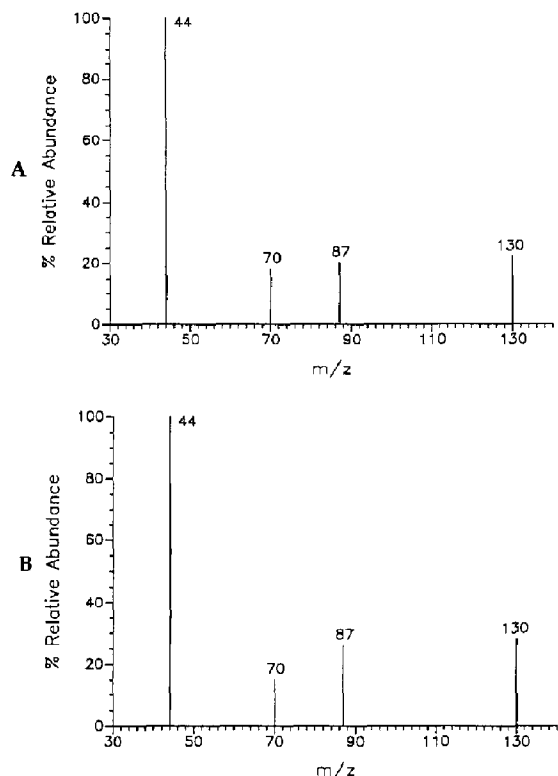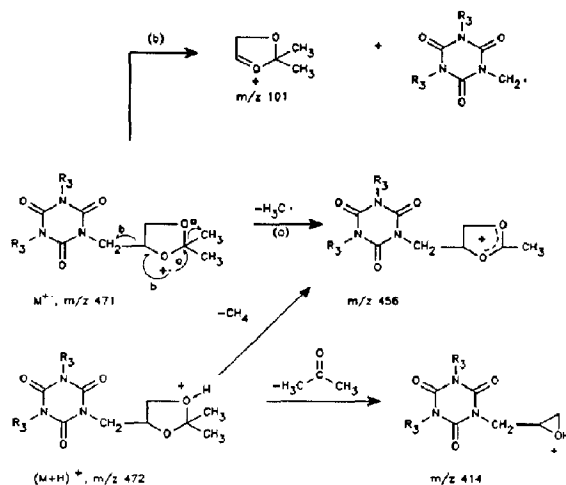**Figure 2.** MS[3] two-dimensional familial scan from Polymer-I.

Figure 3. (a) MS/MS daughter spectrum of m/z 130 from Polymer-I; (b) MS/MS daughter spectrum of protonated cyanuric acid.
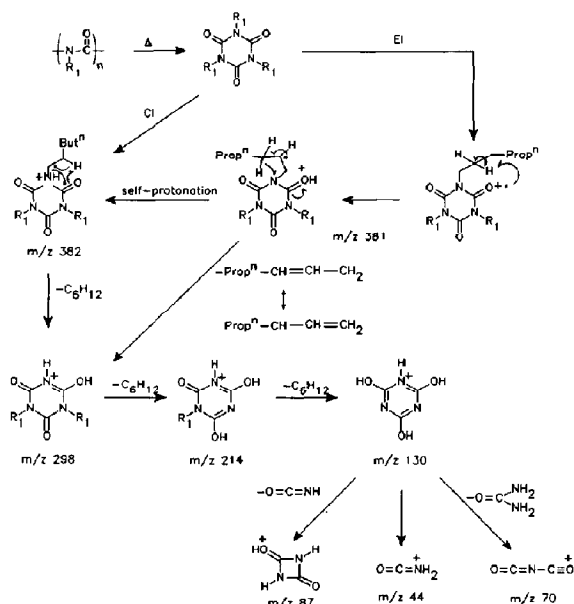

Scheme I

Scheme II

relationship between ions m/z 382 produced from Polymer-I and Polymer-II is confirmed by their different daughter spectra (Tables 2 and S-2).

A significant amount of the protonated trimer of *poly(2,2-dimethyl-1,3-dioxolan-4-yl)methylisocyanate* (Polymer-III) is observed under DCI conditions, at m/z 472 (Table S-3). Under DEI conditions, however, the ionized forms of the trimer are not observed. A major peak in the DEI mass spectrum (m/z 456) corresponds to the loss of a methyl radical from the molecular radical cation, or to the loss of methane from the protonated trimer. This type of fragmentation (Scheme II) is expected to be highly favored in the (2,2-dimethyl-1,3-dioxolan-4-yl)methyl substituent (R_3) [43] and it accounts for the absence of molecular ions. Another fragmentation expected to be favored involves loss of acetone and is also shown in Scheme II.

Singly or in combination, these characteristic fragmentation processes (loss of 15 or 16 and 58 u) and also loss of R_3 as nonene (114 u) are responsible for the majority of the observed fragment ions (Scheme S-I). Parent spectra of the major fragment ions (Table S-4) typically show either the protonated trimer ion m/z 472 or the ion m/z 456 as their precursors. Daughter spectra of ions m/z 472 and m/z 456 are decidedly different, as expected from the argument that charge localization occurs on the cyanuric acid in the former and in the side chain of the latter ion.

Another consequence of the favored modes of fragmentation just discussed is that the characteristic alkene elimination sequence is displayed only weakly in Polymer-III, as seen by the low abundance of the protonated cyclic dealkylated trimer, ion m/z 130. In order to check the influence of the charge-stabilizing dioxolane group on the fragmentation behavior of this trimer, 1,3,5-tris(2-hydroxyethyl)cyanuric acid was chosen as an analogue of this compound. Its DEI (70

eV) and isobutane DCI mass spectra (Figure S-1) show production of the protonated molecular ion and complete absence of the m/z 130 fragment ion. The daughter spectrum of $[M + H]^+$ (Figure S-1c) also fails to show any ion m/z 130. These and other similarities between the pyrolysis mass spectra of Polymer-III (Table S-3) and 1,3,5-tris(2-hydroxyethyl)cyanuric acid (Figure S-1) confirm that the oxygenated side chain is responsible for the distinctive fragmentation pathway of the trimer derived from Polymer-III.

The MS/MS parent spectrum of the ion m/z 101 (Table S-4), a very abundant ion in the DEI spectrum from Polymer-III, does not display any precursors. Its greatly decreased abundance in the DCI mass spectra implies that it is not an ionized form of a pyrolysis product and that it is probably generated by rapid fragmentation of the trimer radical ion in the ion source (Scheme II), as is also the case for ion m/z 456. Although the ion m/z 101 is expected to be less stable than ion m/z 456, its high relative abundance

may be due in part to the formation of the more stable complementary radical product.

Carbon–Carbon bond cleavages. The ion m/z 311, present in the mass and MS/MS spectra of Polymer-I (Tables 1 and 2), appears to be a radical ion and its parent spectrum suggests that it is the product of cleavage of the α C—C bond in $M^{+\cdot}$ with elimination of the elements of neutral pentene. This α-cleavage process may occur by hydrogen atom transfer to the ionized nitrogen in a five-membered ring as shown in Scheme III. A similar process has been reported for N-n-butylsuccinamide [38]. The methyl substituent in the ion m/z 311 shows its presence by the fact that further fragmentation proceeds through ions m/z 241 and 228 and ultimately leads to ions m/z 158 and 144, respectively, rather than giving the lower homologue m/z 130.

The protonated trimer, m/z 382, is also an important precursor of the fragments at m/z 228, 158, and 144, as well as the fragment ion m/z 242, which is the
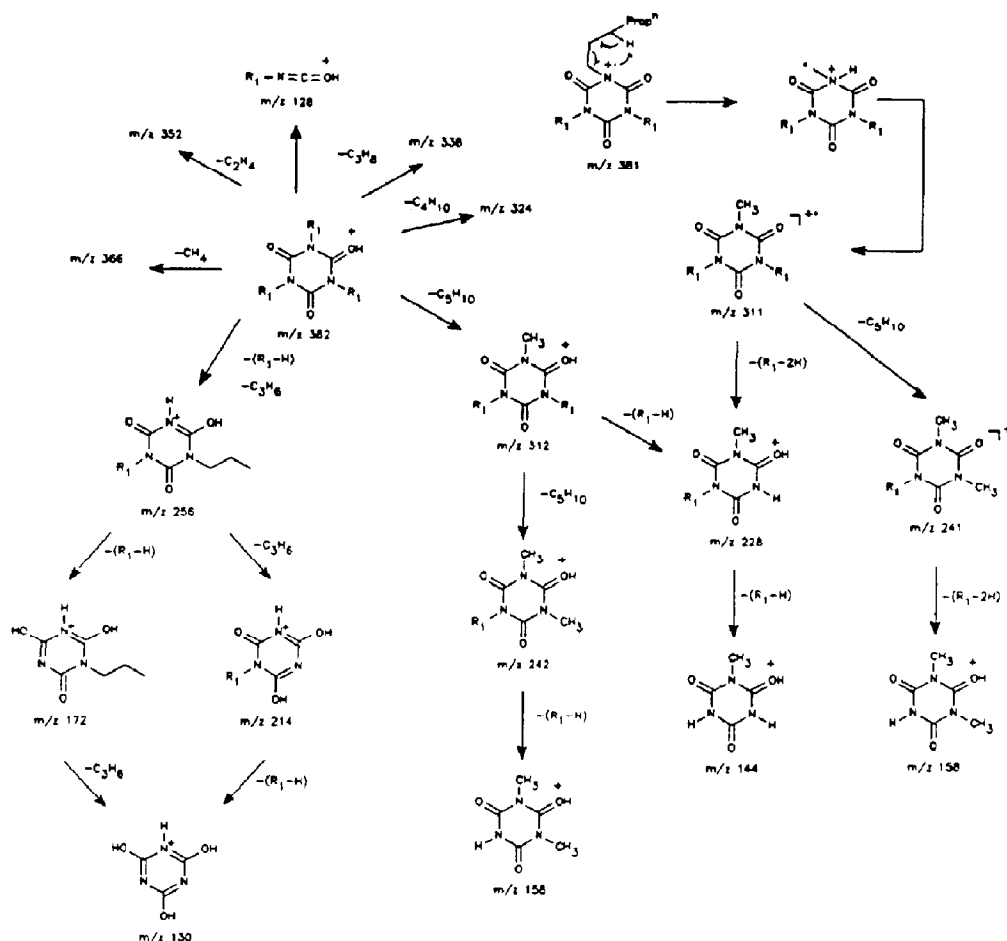

Scheme III

base peak in the parent spectrum of m/z 158. These findings indicate that α C—C bond cleavage also occurs in the protonated trimer (Scheme III).

The daughter spectra of the high-mass ions generated from the pyrolysate of Polymer-II do not show the α C—C bond cleavage intermediate products, although m/z 270 appears in the 70-eV DEI mass spectrum and in the parent spectra of m/z 144, as its

major precursor. On the other hand, ion m/z 298 appears to be a β C—C bond cleavage product. It is formed from ions m/z 382 and 508, by processes that must involve loss of C_6H_{12}, and it fragments to m/z 172 and 130, which suggests a cyanuric acid structure bearing an R_2 substituent and a propyl group. Another possible β C—C cleavage product, ion m/z 424, is one of the parents of the ion m/z 127 (Scheme IV).

Scheme IV
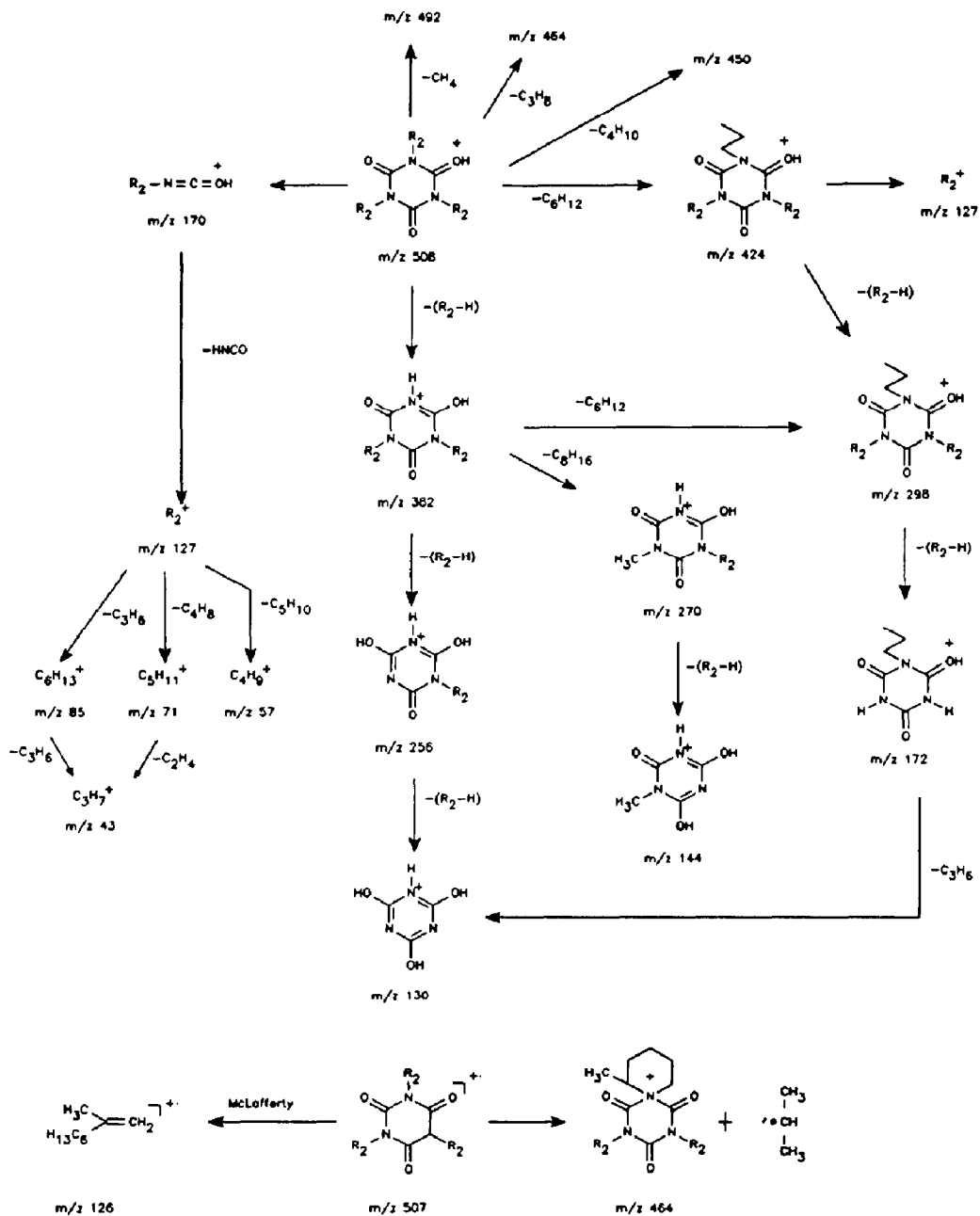
The near absence of the α-cleavage analogue and the presence of β-cleavage products for Polymer-II are accounted for by the presence of the methyl substituent at the β carbon in the R_2 chain. This substituent can stabilize the radical generated at this site upon a six-centered hydrogen transfer to the nitrogen that would occur in a β-cleavage process.

Radical stabilization at the β carbon, within R_2, may also explain the relatively abundant formation of the ionized alkene (m/z 126) in the DEI mass spectra of Polymer-II. This ion can be generated from M^{+} (m/z 507) by a McLafferty-type rearrangement [42] in which the stability of the radical at the β carbon atom leads to retention of the charge by the alkene (Scheme IV).

A protonated cyanuric acid structure bearing a hexyl (R_1) and a propyl group formed by a γ C—C cleavage is attributed to the ion m/z 256 (Scheme III). The protonated cyclic trimer, m/z 382, formed from Polymer-I is the major source of the ion m/z 256. The most important ions in the daughter spectrum of this fragment are m/z 214, 172, and 130 (Table 2). This dissociation pattern indicates the presence of both propyl and hexyl substituents, loss of hexene yielding m/z 172, loss of propene yielding m/z 214, and loss of both groups as alkenes yielding m/z 130.

The DEI mass spectrum of Polymer-II (Table S-1) shows an ion at m/z 464 that may correspond to an ipso cyclic product due to ϵ C—C bond cleavage in the trimer radical cation (m/z 507). This six-centered fragmentation process (Scheme IV) is probably favored by the stability of the isopropyl radical generated. The further fragments corresponding to sequential loss of the R_2 group as nonene from ion m/z 464 are also observed at m/z 338 and 212.

Charge-remote fragmentations. Fragmentation formally remote from the charge site is expected in energetic even-electron ions, such as protonated amides, which bear long-chain alkyl substituents [39, 40]. The DEI and methane DCI mass spectra of Polymer-I display a series of low-abundance ions, m/z 366, 352, 338, and 324, which may arise through charge-remote fragmentation (Table 1, Scheme III). These ions are formally due to alkane loss from the protonated trimer. The fact that they do not appear in any MS/MS spectra may be due to the low collision energy used in these experiments. We consider it unlikely that they are direct pyrolysis products because they should then appear in all the DCI spectra.

The charge-remote fragmentations evident in the n-hexyl case are also apparent in the nonyl case, i.e., Polymer-II. The position of branching of the R_2 chain is discernible in these ions as seen by the fact that the alkane loss sequence is interrupted at C_6; i.e., in the sequence m/z 492, 478, 464, and 450, m/z 478 is absent (Table S-1, Scheme IV).

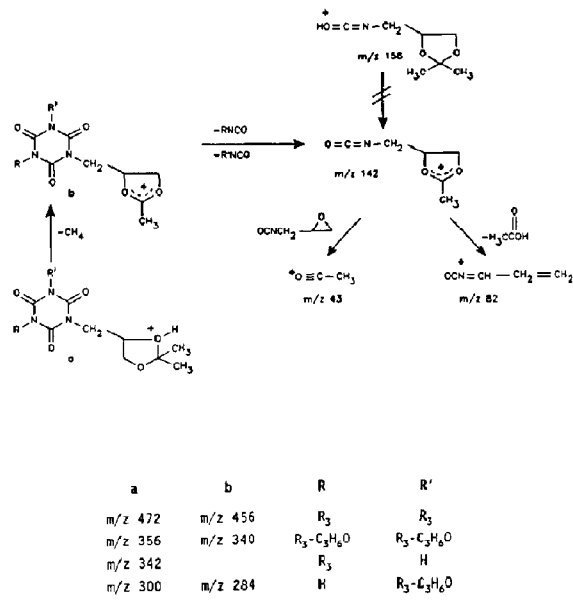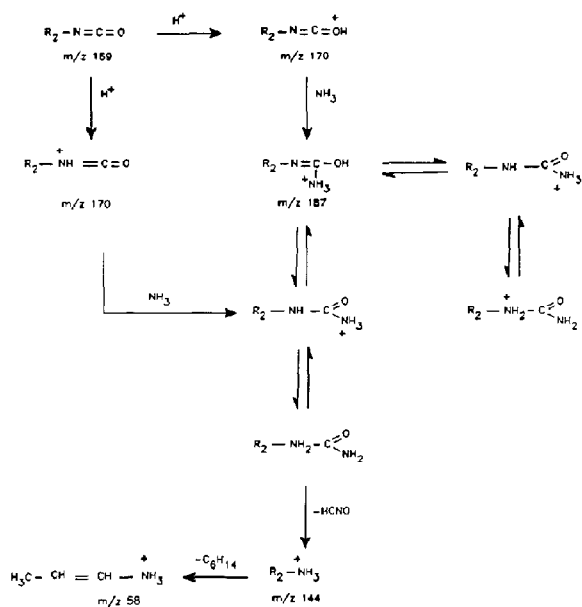The above discussion demonstrates that carbon–carbon bond cleavages within the alkyl chain make a

contribution to the ion chemistry of the pyrolysate of Polymer-I and Polymer-II even though the major reactions are dominated by loss of the hexyl group in the form of hexene.

The protonated monomer. The ion m/z 128, which is very abundant in the methane DCI pyrolysis mass spectrum of Polymer-I, corresponds to protonated n-hexylisocyanate, viz., to the protonated monomer. The fact that its abundance increases as the exothermicity of protonation increases suggests that it is, at least in part, the product of fragmentation of the protonated trimer (Scheme III). The parent spectrum of m/z 128 confirms this view. However, the presence of the isobutane adduct seen at m/z 184 in the isobutane CI mass spectrum provides evidence for direct generation of the monomer as a neutral product of pyrolysis. The daughter spectrum of m/z 184 (Table 2) shows the isobutyl cation at m/z 57 and the protonated monomer at m/z 128 as major fragments. The formation of m/z 128 from m/z 382 requires that there exist a fragmentation pathway of the protonated trimer by a ring opening mechanism to yield the protonated monomer, an expected process.

The second major fragmentation process evident from the mass and MS/MS spectra of the protonated trimer (m/z 508) generated from Polymer-II is the formation of the protonated monomer, m/z 170. The parent spectrum of this ion confirms that it arises, at least in part, as a dissociation product of the protonated trimer. Further fragmentation by HNCO loss to yield R_2^{+} (m/z 127) and its fragments (Scheme IV) is apparent by a comparison of the daughter spectra of ions m/z 170 and 127 (Table S-2). The NH_3 DCI mass spectrum shows the ammonia adducts (m/z 525 and 187) of the protonated trimer (m/z 508) and of the protonated monomer (m/z 170). This result suggests a second route to the monomer, viz., that it is generated separately as a neutral molecule. The alternative, that the [monomer + NH_4]$^{+}$ ion is a fragment of the [trimer + NH_4]$^{+}$ ion was tested by recording the daughter spectrum of the latter (Table S-2). This spectrum shows abundant ions due to the normal alkene loss sequence without retention of the ammonia, m/z 382, 256, and 130. This indicates a weakly bound NH_3, although m/z 382 was accompanied by a low-abundance ammonia adduct at m/z 399. Neither the monomer nor its ammonia adduct was observed, confirming the independent formation of the neutral monomer by pyrolysis.

The daughter spectrum of the ion m/z 144, generated by NH_3 DCI, is distinctly different from that of m/z 144 when generated by DEI (Table S-2). The ion at m/z 144 in the NH_3 DCI mass spectrum is not the product of dissociation of [M + NH_4]$^{+}$, as shown by the daughter spectrum of the latter; however, it is generated from the ammonia adduct of the monomer, and it is therefore concluded that this ion corresponds to the protonated amine [R_2NH_2 + H]$^{+}$. The ammo-

Scheme V

a	b	R	R′
m/z 472	m/z 456	R_3	R_3
m/z 356	m/z 340	R_3-C_3H_6O	R_3-C_3H_6O
m/z 342		R_3	H
m/z 300	m/z 284	H	R_3-C_3H_6O

Scheme VI

nia adduct of the monomer (m/z 187) must be covalently bound, because its dissociation by HCNO loss to yield the protonated alkylamine $R_2NH_3^+$ is suggested by the mass spectrum, confirmed by its daughter spectrum, and accounted for by the mechanism given in Scheme V. Note that there is ample precedent for covalent bond formation upon ammonia addition to multiple bonds, including the formation of Schiff bases in the gas phase [41].

Further evidence for the production of the neutral monomer during pyrolysis of Polymer-II is found in the isobutane DCI mass spectrum. In addition to the protonated monomer, the monomer–isobutane adduct appears at m/z 226. The MS/MS daughter spectra of m/z 226 (Table S-2) show the butyl cation (m/z 57) as the major fragment, along with the protonated monomer, m/z 170.

The fragment ion m/z 158 in the DCI mass spectra of Polymer-III appears to be the protonated isocyanate monomer, and its parent spectrum shows the protonated trimer, m/z 472, and m/z 284 [MH$^+$-114-58] as its major high-mass precursors. Therefore, a pathway in which the trimer fragments to yield the monomer is also operative for Polymer-III just as it is for Polymer-I and Polymer-II. Even more of the protonated monomer (m/z 158) is present in this case (Table S-3) than for the alkyl-substituted polymers, the ratio of protonated monomer to protonated trimer in the CH_4 DCI mass spectrum being 0.4 for the n-hexyl, 9.0 for the nonyl, and 100 for the dioxolane derivative. As also noted for the nonyl polymer, the abundance of the protonated monomer increases relative to that of the protonated trimer as the exothermicity of protonation increases. This, together with direct evidence

from the parent and daughter spectra, establishes the interconnection of these two ions through fragmentation. However, as in the nonyl case, direct production of the neutral monomer by pyrolysis is also indicated here; the NH_3 DCI spectrum shows NH_4^+ adducts of the two suspected neutral pyrolysates, the trimer (m/z 489) and the monomer (m/z 175). Consistent with this, the major fragment of the protonated trimer, m/z 414, shows no ammonia adduct. Note that the isobutene adduct of the protonated monomer (m/z 214) is also present in this polymer. These processes involving formation of the protonated monomer and its adducts are summarized in Scheme S-II.

Other Processes for Polymer-III. The parent spectrum of the abundant fragment ion m/z 142 (Table S-4) indicates the structure shown in Scheme VI. A retro Diels–Alder process is proposed involving loss of two RNCO groups, a process similar to that suggested for monomer formation from the protonated trimer (Scheme S-II). This structure is also consistent with its daughter spectrum. The fact that the protonated monomer (m/z 158) does not lose methane to give the ion m/z 142, in analogy with methane loss from the protonated trimer, suggests that its charge is located on the isocyanate rather than the dioxolane ring. This is consistent with the expected increase in proton affinity of the isocyanate over the cyanuric acid group.

The ion m/z 114, which appears in the DEI mass spectra, is probably [R_3 − H]$^{+\cdot}$. Its formation in relatively good abundance may be explained, in analogy with the formation of the ion m/z 126 from Polymer-II, by the stability of the radical that is formed at the β
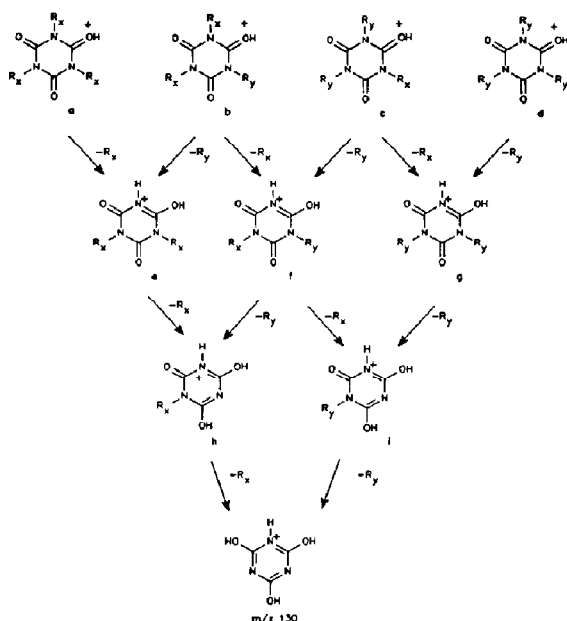
Polymer	R_x	R_y	prot. trimers m/z a	b	c	d	e	fragment ions f	g	h	i
IV	R_1	R_2	382	424	466	508	298	340	382	214	256
V	R_2	R_1	508	522	536	550	382	396	410	256	270
VI	R_1	R_3	382	412	442	472	298	328	358	214	244

Scheme VII

carbon of the R_3 group when fragmentation occurs through a McLafferty-type rearrangement with retention of the charge by the alkene [42]. From the above discussion it is clear that post-ionization fragmentation of thermally decomposed Polymer-III is quite different from the first two polymers because of the presence of the dioxolane substituent.

Copolymers

Major pyrolysis products and fragmentation pathways. Copolymers having two different types of substituents might produce four different trimers upon pyrolysis, each of which can lose their alkyl groups as alkenes to give protonated cyanuric acid, m/z 130, through the fragmentation pathway shown in Scheme VII (R_4 = 3,7-dimethyloctyl group).

Pyrolysis mass spectra of Polymer-IV and Polymer-V display the four protonated trimers at m/z 508, 466, 424, and 382 (Table 3), and at m/z 550, 536, 522, and 508 (Table S-5), respectively. The parent spectra of m/z 130 generated from these copolymers show all four trimers and the expected alkene loss fragments (Figure 4). The isobaric nature of ion m/z 382 in Polymer-IV (Scheme VII) is clearly seen by the reaction intermediate spectrum (Figure 5a), which shows the two competitive routes from ion m/z 382 to protonated cyanuric acid: loss of two C_9H_{18} or loss of three C_6H_{12} molecules.

The alkene loss processes for the asymmetrical protonated trimer, m/z 424, generated from Polymer-IV are revealed with startling clarity in the reaction intermediate spectrum (Figure 5b). This mode of scanning removes contributions from all other processes. It is of interest that one possible process, the loss of two molecules of hexene in sequence (ion m/z 256), is observed in very low abundance in this spectrum. The preferential loss of the larger alkene, i.e., nonene over hexene, can be simply accounted for by the fact that the hydrogen bound to a tertiary carbon in the nonyl group can be transferred more readily than that bonded to a secondary carbon in the n-hexyl group through the mechanism proposed in Scheme I. The reaction intermediate spectrum for the other asymmetrical trimer, m/z 466 (Figure 5c), again shows favored loss of the larger alkene. In this spectrum, only the large alkene loss fragment ions occur at m/z 340 and 214 (Scheme VII). This is also confirmed in the daughter spectrum of ion m/z 340 (Scheme VII, Table 4), which shows a preference of more than 40:1 for loss of the larger alkene (m/z 214) over the smaller (m/z 256). The formation of the same protonated trimer of m/z 508 from this copolymer (Polymer-IV) and from Polymer-II is revealed by the similarity of their reaction intermediate spectra (shown for Polymer-IV in Figure 5d), which display the two expected intermediates (Scheme VII).

The reaction intermediate spectra for the four protonated trimers generated from Polymer-V reveal the fragmentation routes to protonated cyanuric acid as shown in Figure 6. As expected, the two symmetrical trimers, m/z 508 and 550 (Figure 6a and d, respectively), show just the two alkene loss intermediate ions. The asymmetrical nonyl-didecyl trimer, m/z 536, shows three intermediate ions, m/z 410, 396, and 270 (Figure 6c). The competitive losses of nonene and decene yield the first two ions. Remarkably, the sequence m/z 536 ($[M + H]^+$) → 396 → 256 → 130, in which the alkenes lost are, in order, decene, decene, and nonene, is not observed. The fact that the very similar sequences decene, nonene, decene (536 → 396 → 270 → 130) and nonene, decene, decene (536 → 410 → 270 → 130) are observed can nevertheless be readily explained by the fact that nonene but not decene loss can occur by transfer of a hydrogen bound to a tertiary carbon, through the mechanism shown in Scheme I. Note that the missing ion m/z 256 does occur in the mass spectrum (Table S-5), and its MS/MS daughter and parent spectra (Table S-6) show that this ion does fragment to yield m/z 130 and that it does arise from m/z 536. Corresponding selectivity is observed in the reaction intermediate spectrum of the other asymmetrical trimer, m/z 522 (Figure 6b).

The protonated tri(n-hexyl) trimer (m/z 382) is the only trimer observed in both the 70-eV and the 15-eV DEI pyrolysis mass spectra of Polymer-VI (Table S-7). The protonated singly and doubly R_3(dioxolane group)-substituted trimers (m/z 442 and 412) are ob-

Table 3. Direct pyrolysis mass spectra of Polymer-IV, obtained with different ionization methods[a]

	DEI methods		DCI methods		
m/z	70 eV	15 eV	NH$_3$	i-butane	CH$_4$
525	—	—	8	—	—
508	1	2	—	7	4
483	89	—	45	—	—
466	12	11	28	47	34
452	—	—	—	—	7
441	—	—	100	—	—
424	30	23	60	100	100
408	—	1	—	—	9
399	—	—	65	—	—
382	28	20	40	71	71
381	8	7	—	—	—
366	1	2	—	—	4
352	2	2	—	—	1
340	48	66	—	1	4
323	3	3	—	—	—
311	2	2	—	—	—
298	100	100	2	2	5
281	3	2	—	—	—
254	1	—	—	—	—
256	4	—	—	—	—
242	2	—	—	—	—
228	8	—	—	—	—
226	—	—	—	8	—
214	13	—	—	—	—
184	—	—	—	5	—
183	2	—	—	—	—
170	4	—	—	3	30
154	2	—	—	—	2
144	5	—	1	—	—
130	16	—	2	—	—
128	—	—	—	6	61
126	11	3	—	—	20
113	11	3	—	13	3

[a]Isotopic peaks and ions less than 1% in relative abundance are not reported.
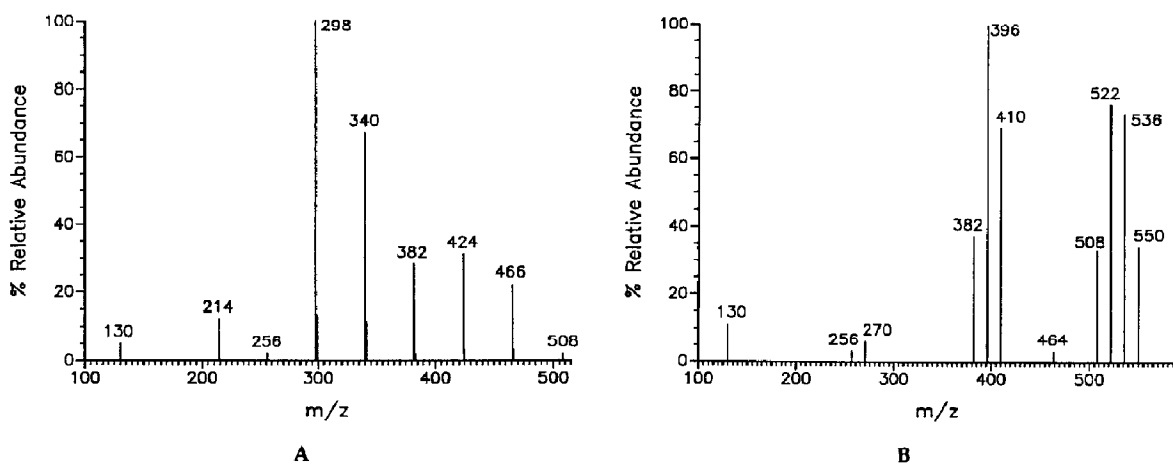
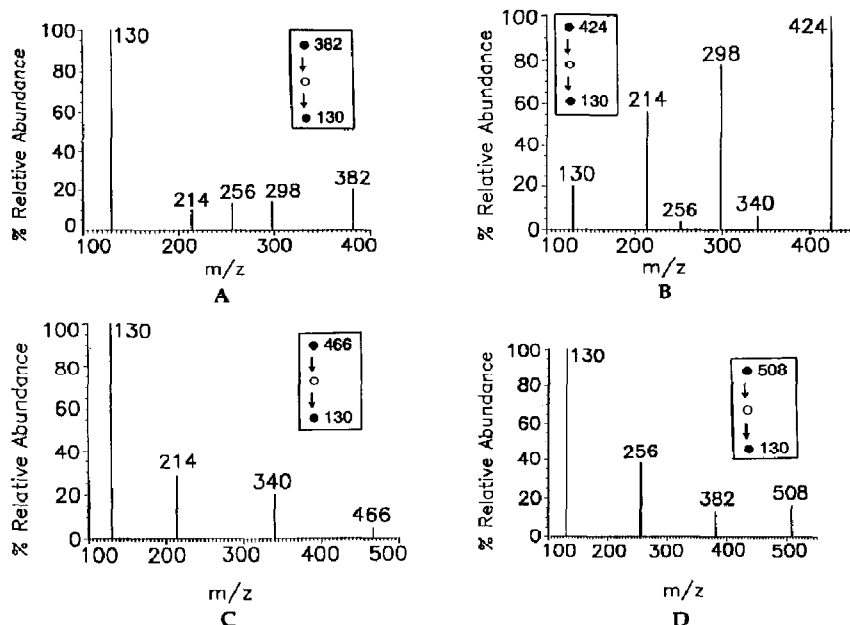**Figure 4.** MS/MS parent spectrum of m/z 130 from Polymer-IV and Polymer-V.

Figure 5. MS^3 reaction intermediate spectra of the protonated trimers at (a) m/z 382, (b) m/z 424, (c) m/z 466, and (d) m/z 508, from Polymer-IV.

served only in low abundance in the 15-eV DEI spectrum, and the protonated tri-R$_3$-substituted trimer (m/z 472) is not observed in any DEI spectra. This is not surprising, because the protonated trimer expected for Polymer-III was not observed in its DEI spectra either. The ions at m/z 456, 426, and 396, which are formally either the methyl radical loss products from the molecular ion or the products of methane

loss from the protonated trimers m/z 472, 442, and 412, respectively, are observed in both DEI spectra. However, formation during pyrolysis of all four intact protonated trimers and two different monomers (m/z 128 and 158) is evident from the methane and isobutane DCI spectra (Table S-7), which display these ions at high abundance. Daughter spectra of each of these ions (Table S-8) are consistent with the fact that they
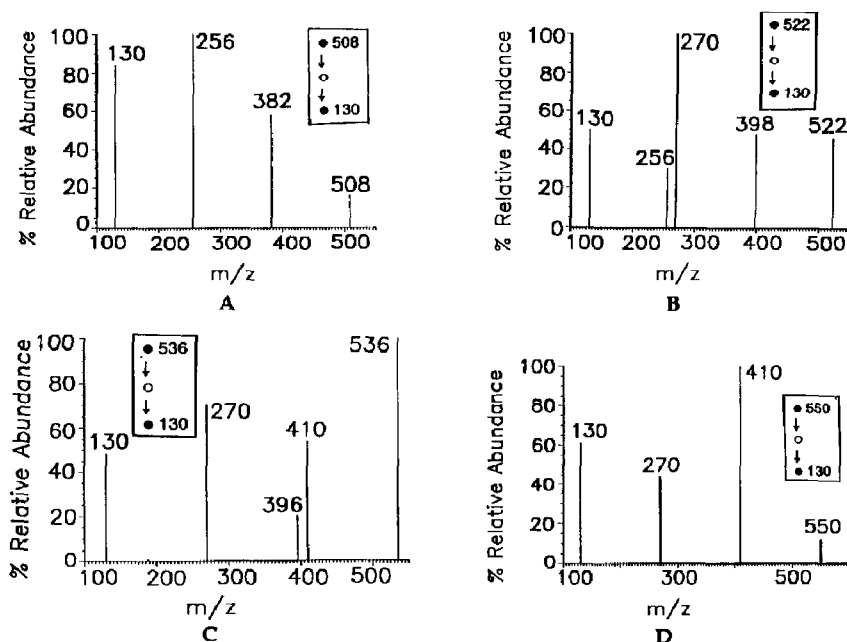

Figure 6. MS^3 reaction intermediate spectra of the protonated trimers at (a) m/z 508, (b) m/z 522, (c) m/z 536, and (d) m/z 550, from Polymer-V.

Table 4. MS/MS spectra of the major ions of Polymer-IV[a]

Selected ion m/z	Daughter ions m/z (% relative abundance)	Parent ions m/z (% relative abundance)
525[b]	508(100), 382(91), 256(16), 130(13)	None observed
508	464(1), 382(50), 256(72), 170(18), 144(6), 130(100), 85(40), 71(15)	525(100)[b]
483[b]	466(94), 340(100), 214(67), 130(81)	None observed
466	340(75), 214(100), 170(8), 130(85), 85(30), 71(22)	483(100)[b]
441[b]	424(61), 340(6), 315(1), 298(100), 214(29), 130(4)	None observed
424	340(15), 298(100), 256(2), 214(66), 170(3), 130(88), 85(32), 71(12)	441(100)[b]
399[b]	382(100), 315(1), 298(95), 214(46), 130(13)	None observed
382	298(46), 256(6), 214(42), 130(100), 128(23), 87(3), 85(81), 71(10), 57(5), 43(7)	466(19), 508(100), 399(100),[b] 525(1)[b]
340	256(1), 214(43), 130(100), 85(19), 71(13), 57(7), 43(3)	466(100), 424(8)
298	214(20), 130(100), 87(8), 85(6), 59(1), 57(7), 43(14)	424(100), 408(2), 382(37)
256	214(4), 172(5), 130(100), 87(19), 85(6), 71(17), 70(2), 57(10), 43(37)	508(39), 492(22), 479(5), 466(56), 424(40), 382(100), 340(72)
228	144(100), 101(4), 87(11), 70(2), 57(42), 43(32)	382(100), 366(10), 311(85)
226	170(7), 85(12), 71(25), 57(100), 43(100), 41(4), 29(2)	None observed
214	130(100), 87(38), 85(5), 70(5), 59(3), 57(14), 43(98)	466(40), 424(100), 382(30), 340(39), 298(41)
184	142(1), 128(4), 85(31), 57(100), 43(61), 41(9), 29(3), 27(2)	None observed
170	127(11), 87(15), 85(9), 71(75), 58(73), 55(98), 43(100)	508(30), 466(27), 442(3), 424(100), 382(19), 340(3), 338(22), 310(5)
144[c]	87(10), 70(5), 59(92), 57(3), 43(100)	508(6), 466(4), 424(5), 396(53), 382(9), 354(40), 312(100), 298(6), 282(11), 270(19), 228(98), 214(8), 186(16)
130[c]	87(4), 70(6), 43(100)	508(3), 466(20), 424(31), 382(30), 340(67), 298(100), 256(2), 214(6)
126[c]		466(35), 424(20), 382(55), 324(100), 170(59)

[a] Conditions: Isobutane DCI (unless otherwise noted), 20-eV collisions on Argon (2 mtorr).
[b] Ammonia DCI is used.
[c] 70-eV DEI is used.

represent the four intact protonated trimers, where loss of acetone produces the more abundant fragment ions from the dioxolane-substituted protonated trimers, m/z 414, 384, and 354, respectively. The alkene elimination sequence ending at m/z 130 (Scheme VII) is also observed. Daughter spectra of ions m/z 382, 298, 256, 214, 158, 144, and 130 are

similar to those observed for the ions having the same mass-to-charge ratio from Polymer-I (Table 2). Therefore, these ions have the structures described in Schemes I and III. The ion m/z 101 observed for Polymer-III (Scheme II) is also present in high relative abundance in the DEI mass spectrum of this copolymer.

Carbon–Carbon bond cleavages. The occurrence of these processes is observed in the mass and MS/MS spectra of Polymer-IV and Polymer-V. The 70-eV DEI spectrum for Polymer-IV displays three expected α-cleavage ions, m/z 311, 228, and 144. The parent spectrum of ion m/z 144, the N-methyl homologue of m/z 130, displays all four protonated trimers, along with all the N-methylated precursors, m/z 396, 354, 312, 270, and 228. The α-cleavage is clearly shown for Polymer-V by the presence in the mass and MS/MS spectra (Tables S-5 and S-6) of the N-methyl cyclic terminal ions, m/z 144 and 158, and their precursors, ions m/z 270, 284, 298, 396, 410, and 424 (Scheme VIII). The preferential α-cleavage in R_4 over R_2 is expected from the fact that R_2 has a methyl group at the β-carbon, as discussed for Polymer-II, and is evident from the fact that m/z 424, 410, and 396 are not displayed in the daughter spectra of the protonated trimers m/z 536, 522, and 508, respectively. These fragmentations would involve α-cleavage in R_2 and loss of pentene. This process is observed only to a small extent and is exemplified by the presence of the protonated tri-R_2-substituted trimer (m/z 508) in the parent spectrum of m/z 144.

It is interesting to note that the R_2 ε-cleavage products are observed in the DEI mass spectra of Polymer-V (m/z 492, 478, and 464), but the corresponding R_4 product (m/z 506) is missing. This process for R_4 would involve loss of the same stable isopropyl radical as for R_2 but would occur via a seven- rather than a six-membered intermediate.

That ions m/z 270, 396, and 410 from Polymer-V each consist of two isobars, one originating by α C—C cleavage and the other by the alkene loss sequence (Scheme VII), is confirmed by their daughter spectra, which display the two expected cyclic termi-

nal ions, m/z 144 and 130. In the same way, the occurrence of two isobaric forms of the ion m/z 284, one having one methyl substituent and the other having two, is evident in its daughter spectrum, which displays both the mono- (m/z 144) and the dimethylated (m/z 158) cyclic ions. Furthermore, the occurrence of two isobaric forms of the ion m/z 298, one due to the double α C—C cleavage product (Scheme VIII) and the other to the β C—C cleavage product from m/z 508 (Scheme IV), is evident in its MS/MS daughter spectrum. The daughter spectrum of this ion displays both the cyclic dimethylated ion m/z 158 and the daughter ions expected from the β-cleavage, ions m/z 172 and 130.

Charge-remote fragmentation. This process is seen to a very small extent in the DEI mass spectra of Polymer-IV and Polymer-V. Polymer-IV displays only ion m/z 408, which can be formed by this process. Ions m/z 492, 478, and 464 for Polymer-V, which have been assigned as ε-cleavage products, can also be generated from the protonated trimer by charge-remote fragmentation.

Protonated monomers. The ions m/z 184 and 226 in the isobutane spectrum for Polymer-IV are the isobutane adducts of the monomers discussed in connection with Polymer-I and Polymer-II, respectively. The ion m/z 170 has the same daughter spectrum as that observed for the ion of the same mass generated from Polymer-II (Table S-2), which indicates that m/z 170 is the protonated monomer of 2,6-dimethylheptylisocyanate.

The MS/MS data for m/z 184 (R_4NCOH^+) and m/z 170 (R_2NCOH^+) observed in the DCI mass spectra of Polymer-V (Table S-5) suggest that they are the protonated monomers. Their parent spectra display the intact trimers as precursors. Formation of monomers during pyrolysis is also evident from the generation of isobutene adducts of the monomers, observed at m/z 226 and 240, during isobutane DCI (Table S-5).

The isobutene adducts of the monomers discussed earlier in the cases of Polymer-I and Polymer-III are also present for Polymer-VI at m/z 184 and 214 following isobutane DCI (Table S-7). The ion m/z 214 observed during 70-eV DEI is isobaric with the ion m/z 214 observed during isobutane DCI, which is clear from the MS/MS spectra shown in Table S-8.

Other processes. As seen in other cases, the ammonia DCI mass spectrum of Polymer-VI (Table S-7) also shows direct evidence for the generation of the neutral trimer molecules in the form of the ammonia adducts, m/z 489 (472 + 17), m/z 459 (442 + 17), m/z 429 (412 + 17), and m/z 399 (382 + 17). The ammonia adduct of one monomer is also observed at
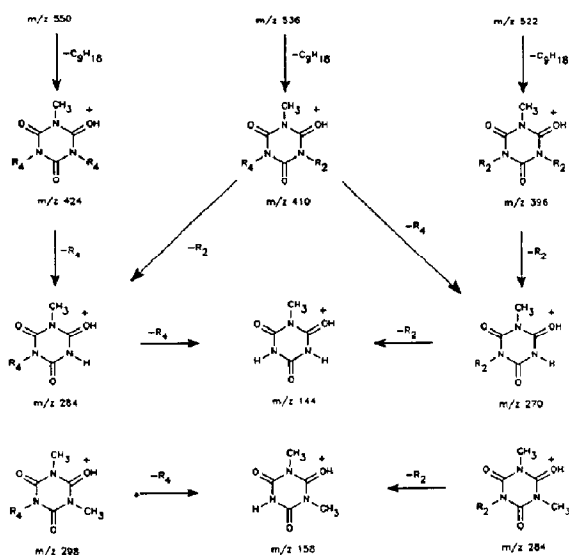
Scheme VIII

Scheme IX
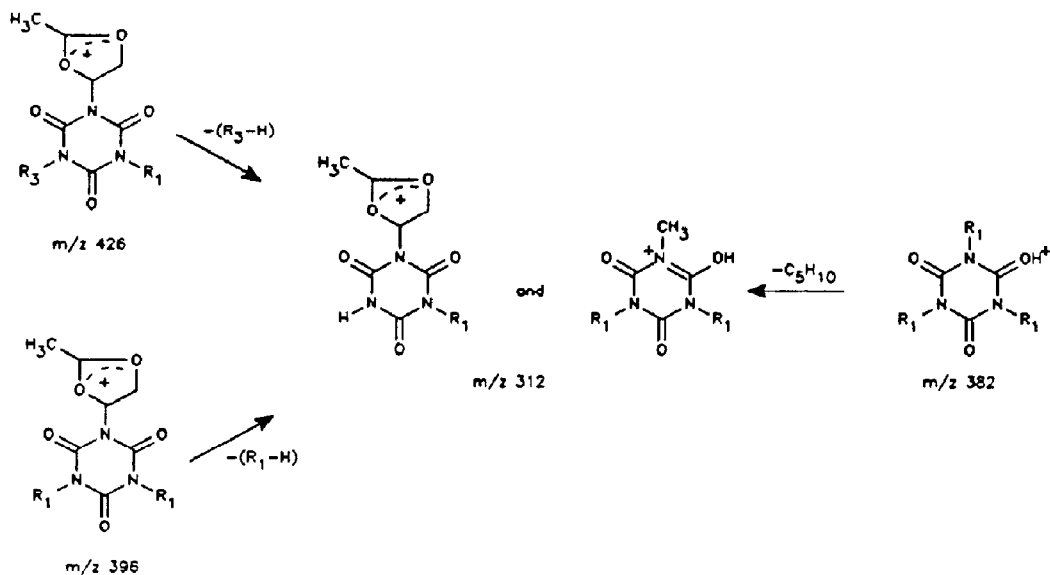
m/z 175 (158 + 17), as well as ammonia adducts of the fragment ions m/z 426 (m/z 443) and m/z 396 (m/z 413). These two latter adducts appear to be formed by loss of 46 (from the trimers m/z 472 and 442, respectively). This reaction was not encountered in the homopolymers and is therefore ascribed to combined loss of 16 and 30 u due to fragmentation involving participation of both the R_3 and R_1 chains. The ion m/z 473, which is the ammonia adduct of m/z 456, was also observed although in low abundance. These low-abundance ammonia adducts of fragment ions are significant, since they may indicate a covalently bound ammonium adduct of the trimer, although they could also be formed from the fragments themselves in the ion source. This result also contrasts with that observed for the homodioxolane polymer (Polymer-III) where fragmentation of the ammonia trimer adduct led overwhelmingly to loss of ammonia.

The MS/MS daughter spectra of m/z 312 for Polymer-VI (Table S-8) indicate the existence of two isobars: the first produced from m/z 426 by the loss of nonene and from m/z 396 by the loss of hexene, and the second derived from the protonated n-hexylisocyanate trimer (m/z 382) by β-cleavage, as shown in Scheme IX. The MS/MS data on the ion m/z 270 (Table S-8) is best interpreted by assigning three different cyclic structures for this ion formed by the fragmentation pathways shown in Scheme X.

The parent spectrum of m/z 354 shows only m/z 412 as its precursor, and its daughter spectrum shows m/z 298 as the most abundant fragment, as well as other fragments at m/z 270, 214, 186, and 130. It is therefore evident from the MS/MS data that this ion (m/z 354) is formed from m/z 412 by loss of acetone

and that it fragments to m/z 130 by the routes suggested in Scheme XI.

Distribution of Monomers

It is of interest to test the capabilities of mass spectrometry to determine the distribution of monomers in a copolymer. In the case of the polyalkylisocyanates, NMR methods are available although they require relatively large amounts of sample [36, 37]. In the case of a random distribution of monomers, the probabilities of forming different trimer ions can be estimated by simple statistics, considering only the monomer ratio used during synthesis of the copolymer. The theoretical distribution can be calculated by the general formula:

$$P = {}^m C_a{}^n C_b /^{(m+n)} C_{(a+b)}$$

i.e.,

$$P = [\{m!/a!(m - a)!\}\{n!/b!(n - b)!\}] / [(m + n)!/(a + b)!(m + n - a - b)!]$$

where

P = probability of observing a particular trimer,

m = proportion of the first monomer,

n = proportion of the second monomer,

a = number of first monomer groups in the trimer, and

b = number of second monomer groups in the trimer.

The measured distribution of trimers was simply calculated by using the formula $x_i / \Sigma(x_i)$, where x_i = percent relative abundance of the individual trimer ions. Because the theoretical calculation shown above is based on a random distribution of monomers,
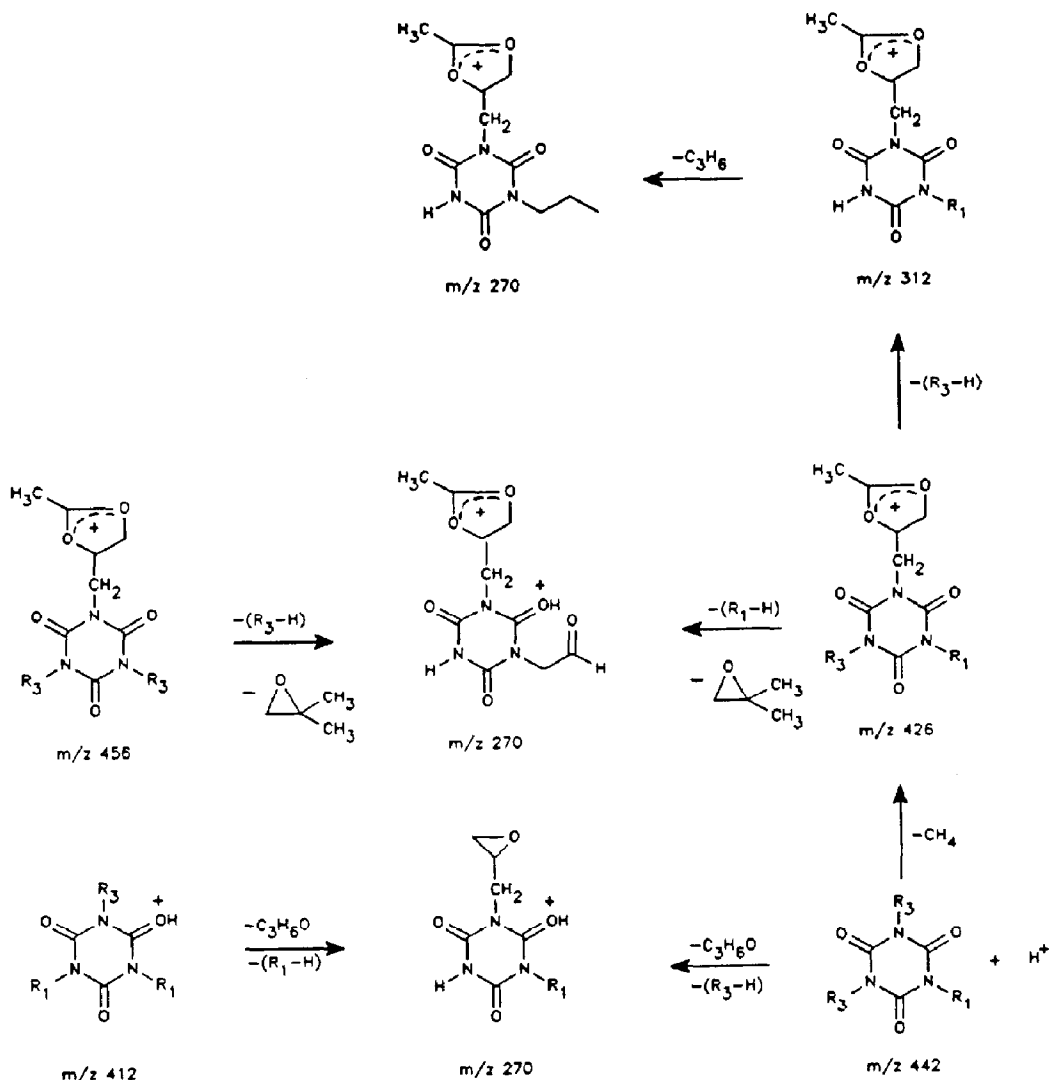
Scheme X

agreement between the experimental data and the theoretical data would imply a random distribution; otherwise the distribution must be nonrandom.

To use the above approach one must be confident that the ion abundances of the protonated trimers reflect the relative proportions in which the neutral trimers are generated. There are three potential sources of error: (1) the relative rates of protonation, (2) the occurrence of processes in the neutral or ion that might lead to scrambling of the substituents or other distortions of the distribution, and (3) differential rates of fragmentation, which would have the same effect. The rates of protonation are taken to be equal, given the similarities expected for proton affinities of the various substituted cyanuric acids. To test the second point, pyrolysis mass spectra were recorded on mixtures of homopolymers under both DEI and DCI conditions. Several different mixtures in different proportions were examined and the results, collected in Table S-9, show that no trimer with mixed substituents was formed. This eliminates the occurrence of substituent interchange in the neutral or in the ionic state. That the third requirement is not completely satisfied is evident from the results presented so far. Correction of the mass spectra for the effects of different rates of fragmentation could be done in principle by summing all ions derived from the particular protonated trimer. This is difficult because the different trimers in a mixture give many common fragments, including isobaric ions of the same nominal mass. This led to the adoption of a method in which each substituent was assigned a

Scheme XI
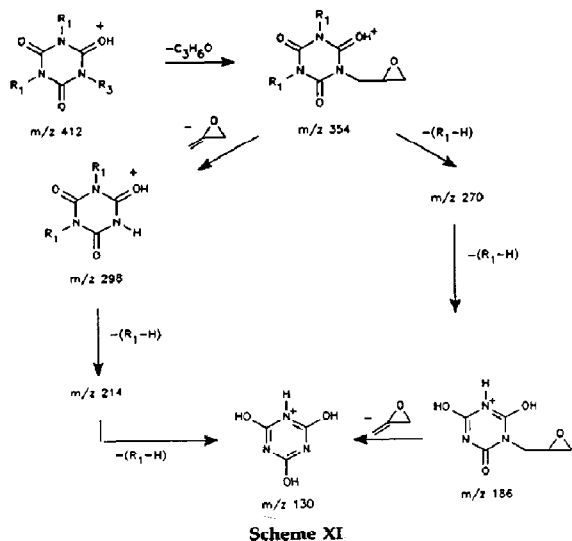
dissociation efficiency, viz., the substituent dissociation efficiency, $R_x \equiv MH^+ / \Sigma F_i^+$, which was evaluated by measuring the extent of dissociation of the corresponding protonated homotrimer under standard MS/MS conditions. A dissociation efficiency for each protonated trimer was then estimated by arithmetically averaging the substituent values. The dissociation efficiency values of the different trimers are included in Table 5 as correction factors. Correction for dissociation of the ionized copolymers was performed by multiplying the relative abundance of each trimer by the reciprocal of the correction factor. The corrected probabilities of formation of each of the trimers are reported in Table 5, together with the uncorrected values for each copolymer. The theoretical values, which assume a random distribution, are given under the heading "Calculated probability." Because of extensive dissociation at high energy, the corrected protonated trimer abundance was least reliable with the 70-eV DEI data; therefore only the 15-eV data are recorded.

The 15-eV DEI data for Polymer-IV and Polymer-V

agree well with the theoretical values expected for a random distribution of the monomers. This is in agreement with NMR results, which are not readily applied to copolymers in which the alkyl side chains are homologous [36, 37]. Variations could arise due to the implicit assumption that the interactions between the substituents have negligible kinetic effects, both in the formation of the neutral trimers from the polymer and in the dissociation of the ion. In Polymer-IV one would expect isobaric interference for the trimer m/z 382 (discussed earlier) to give an erroneous result in the calculation of the monomer distribution. As we see in Table 5, the experimental results agree well with the calculated results, which proves that the isobaric interference for m/z 382 is negligible under low-energy ionization conditions and that the majority of the m/z 382 ions are the protonated tri(n-hexyl)isocyanate trimer. Another reason for the negligible isobaric effect is that the copolymer contains approximately two n-hexyl groups for every 2,6-dimethylheptyl group, and the rate of fragmentation of the trimers m/z 508 → 382 and m/z 382 → 298 is much slower in the copolymer than in the homopolymers (evident from the abundance ratio of 382/508 at 15-eV DEI in Tables S-1 and 3, of 298/382 at 15-eV DEI in Tables 1 and 3).

Polymer-V was chosen to further test the validity of the methodology by examining slightly different side chains. The nonyl and decyl groups in these copolymers are expected to behave nearly identically. Excellent agreement between experimental and calculated values for this monomer confirms these expectations.

The experimental data for Polymer-VI do not fit well with a random distribution model. There could be several reasons for this, most being related to the unusual ion chemistry of the dioxolane side chain, which makes ions derived from this compound extremely reactive by routes not available to the other polymers and for which the simple correction used may be a poor approximation. Note that the 15-eV DEI spectra of Polymer-VI (Table S-7) do not show the protonated homotrimer m/z 472, and the proto-

Table 5. Distribution of monomers in the copolymers, based on 15-eV DEI data

Copolymer	Trimer (m/z)	Calculated probability	Correction factor	Probability (experimental) Corrected	Probability (experimental) Uncorrected
Polymer-IV	382	0.2456	12.60	0.2530	0.3584
	424	0.4469	18.41	0.4252	0.4122
	466	0.2595	24.22	0.2675	0.1971
	508	0.0481	30.03	0.0543	0.0323
Polymer-V	382	0.6786	12.60	0.6675	0.6102
	396	0.2841	10.40	0.2755	0.3051
	426	0.0359	8.20	0.0483	0.0678
	456	0.0014	6.00	0.0088	0.0169
Polymer-VI	508	0.1212	30.03	0.1163	0.1212
	522	0.3788	31.02	0.3604	0.3664
	536	0.3788	32.01	0.3874	0.3817
	550	0.1212	33.00	0.1358	0.1298

nated trimers m/z 442 and 412 are not abundant. Therefore, in the calculation of the substituent dissociation efficiency we had to use m/z 456, 426, and 396, formed by loss of methyl radical from the radical cations m/z 471, 441, and 411, which are not observed in the mass spectra because of their instability. Such an approximation clearly adds to the error in the method.

Conclusions

Common features in the direct pyrolysis mass spectra of all the polymers discussed above are (1) trimers are the major products of thermal decomposition, along with minor amounts of monomers; (2) the trimers are observed as the protonated molecule and in some cases as the ammonia adduct, and as the radical cation and/or the product of its fast demethylation, depending upon the ionization conditions and the nature of the substituents; (3) the dominant fragmentation of the protonated trimers occurs via sequential losses of the substituents as alkenes, and this yields the key fragment, protonated cyanuric acid at m/z 130; (4) other fragmentation processes include carbon–carbon and charge-remote C—C cleavages within the substituent, which are diagnostic of branching in the alkyl chain; (5) protonated trimers bearing n-hexyl and 2,6-dimethylheptyl substituents show preferential loss of the larger alkyl group, whereas protonated trimers with 2,6-dimethylheptyl and 3,7-dimethyloctyl groups show preferential loss of the smaller alkyl group, both results being explained by preferential transfer of hydrogen bound to a tertiary carbon as opposed to a secondary carbon; (6) the protonated monomer is generated in part by fragmentation of the trimer, a process evident from parent spectra and the increase of the monomer/trimer ratio with increased internal energy deposited upon ionization; (7) the protonated monomer is a substituted urea and accordingly fragments by HNCO loss to yield the protonated amine; and (8) the dioxolane-containing polymer shows fragmentation pathways different from those of the alkyl polymers because of the fragmentation-directing character of the ketal group.

A new approach to estimating the distribution of monomers along the copolymer chain is used in this study. With the possible exception of the copolymer containing the dioxolane substituent, the monomers in the copolymers are distributed randomly along the polymer chain.

Supplementary Material

Supplementary material for this article is available in photocopy form from the office of the Editor-in-Chief (see front of journal for address). Requests must in-clude complete title of article, names of authors, issue date, and page numbers. The supplementary material consists of Figure S-1, Tables S-1 through S-9, and Schemes S-I and S-II.

Acknowledgments

References

1. Shashoua, V. E.; Sweeny, W. E.; Teitz, R. F. *J. Am. Chem. Soc.* **1960**, *82*, 866.
2. Libson, S.; Andreola, C.; Peterson, N. C.; Green, M. M. *J. Am. Chem. Soc.* **1989**, *111*, 8850; and references therein.
3. Bur, A.; Fetters, L. J. *Chem. Rev.* **1976**, *76*, 727.
4. Itou, T.; Teramoto, A. *Macromolecules* **1988**, *21*, 2225.
5. Durairaj, B.; Dimock, A. W.; Samulski, E. T.; Shaw, M. T. *J. Polym. Sci.* Part A: Polymer Chemistry, **1989**, *27*, 3211.
6. Lattimer, R. P.; Münster, H.; Budzikiewicz, H. *Int. J. Mass Spectrom. Ion Processes* **1989**, *90*, 119.
7. Montaudo, G.; Scamporrino, E.; Vitalini, D. *Macromolecules* **1989**, *122*, 623.
8. Bletsos, I. V.; Hercules, D. M.; Vanleyen, D.; Benninghoven, A.; Karakatsanis, C. G.; Rieck, J. N. *Anal. Chem.* **1989**, *61*, 2142.
9. Macfarlane, R. D.; Hill, J. C.; Jacobs, D. L.; Phelps, R. G. In *Mass Spectrometry in the Analysis of Large Molecules*; McNeal, C. J., Ed.; Wiley: Chichester, 1986; p 1.
10. Barber, M.; Green, B. N. *Rapid Commun. Mass Spectrom.* **1987**, *1*, 80.
11. Karas, M.; Bahr, U.; Hillenkamp, F. *Int. J. Mass Spectrom. Ion Processes* **1989**, *92*, 231.
12. Cottrell, J. S.; Greathead, R. J. *Mass Spectrom. Rev.* **1986**, *5*, 215.
13. Amster, I. J.; McLafferty, F. W.; Castro, M. E.; Russell, D. H.; Cody, R. B. Jr.; Ghaderi, S. *Anal. Chem.* **1986**, *58*, 483.
14. Karas, M.; Bahr, U.; Ingendoh, A.; Hillenkamp, F. *Angew. Chem.* **1989**, *101*, 805.
15. Kaiser, R. E.; Louris, J. N.; Amy, J. W.; Cooks, R. G. *Rapid Commun. Mass Spectrom.* **1989**, *3*, 225.
16. Zemany, P. D. *Anal. Chem.* **1952**, *24*, 1709.
17. Plage, B.; Schulten, H. R. *Macromolecules* **1988**, *21*, 2018.
18. Ballistreri, A.; Garozzo, D.; Maravigna, P.; Montaudo, G. *J. Polym. Sci. Polym. Chem. Ed.* **1987**, *25*, 1049.
19. Haken, J. K.; Tan, L. *J. Polym. Sci. Polym. Chem. Ed.* **1988**, *26*, 1315.
20. Ballistreri, A.; Garozzo, D.; Giuffrida, M.; Montaudo, G. *Polym. Degrad. Stab.* **1986**, *16*, 337.
21. Montaudo, G.; Schamporrino, E.; Puglisi, G.; Vitalini, D. *J. Polym. Sci. Polym. Chem. Ed.* **1987**, *25*, 475.
22. Schulten, H. R.; Lattimer, R. P. *Mass Spectrom. Rev.* **1984**, *3*, 231.
23. Snyder, A. P.; Kremer, J.H.; Meuzelaar, H. L. C.; Windig, W.; Taghizadeh, K. *Anal. Chem.* **1987**, *59*, 1945.

24. Mantese, J. V.; Catalan, A. B.; Mance, A. M.; Hamdi, J. A.; Micheli, J. L.; Sell, J. A.; Meyer, M. S. *Appl. Phys. Lett.* **1988**, *53*, 1335.

25. Meuzelaar, H. L. C.; Windig, W.; Huff, S. M.; Richards, J. M. *Anal. Chim. Acta* **1986**, *190*, 119.

26. Cotter, R. J. *Anal. Chem.* **1980**, *52*, 1589A.

27. Pachuta, S. J.; Cooks, R. G. *Chem. Rev.* **1987**, *87*, 647.

28. Nuwaysir, L. M.; Wilkins, C. L.; Simonsick, W. J. Jr. *J. Am. Soc. Mass Spectrom.* **1990**, *1*, 66.

29. Busch, K. L.; Cooks, R. G. In *Tandem Mass Spectrometry*; McLafferty, F. W., Ed.; Wiley: New York, 1983; chap. 2.

30. Busch, K. L.; Glish, G. L.; McLuckey, S. A. *Mass Spectrometry/Mass Spectrometry: Techniques and Applications of Tandem Mass Spectrometry*; VCH Publishers: New York, 1988.

31. Hunt, D. F.; Bone, W. M.; Shabanowitz, J.; Rhodes, J.; Ballard, J. M. *Anal. Chem.* **1981**, *53*, 1704.

32. Bradley, C. V.; Williams, D. H.; Hanley, M. R. *Biochem. Biophys. Res. Commun.* **1982**, *104*,, 1223.

33. Louris, J. N.; Wright, L. G.; Cooks, R. G.; Schoen, A. E. *Anal. Chem.* **1985**, *57*, 2918.

34. Beaugrand, C.; Devant, G.; Jaouen, D.; Rolando, C. *Int. J. Mass Spectrom. Ion Processes*, in press.

35. Schwartz, J. C.; Schey, K. L.; Cooks, R. G. *Int. J. Mass Spectrom. Ion Processes*, **1990**, *101*, 1.

36. Green, M. M.; Gross, R. A.; Crosby, C. C. III; Schilling, F. C. *Macromolecules* **1987**, *20*, 992.

37. Green, M. M.; Reidy, M. P.; Johnson, R. D.; Darlino, G.; O'Leary, D. J.; Willson, G. *J. Am. Chem. Soc.* **1989**, *111*, 6452.

38. Budzikiewicz, H.; Djerassi, C.; Williams, D. H. *Mass Spectrometry of Organic Compounds*; Holden-Day: San Francisco, 1967; chapter 6, section 9.2, p 363.

39. Lyon, P. A.; Crow, F. W.; Tomer, K. B.; Gross, M. L. *Anal. Chem.* **1984**, *56*, 2278.

40. Jensen, N. J.; Tomer, K. B.; Gross, M. L. *J. Am. Chem. Soc.* **1985**, *107*, 1863.

41. Burinsky, D. J.; Campana, D. E.; Cooks, R. G. *Int. J. Mass Spectrom. Ion Processes* **1984**, *62*, 303.

42. McLafferty, F. W. *Interpretation of Mass Spectra*, 2nd ed.; W. A. Benjamin: London, 1973; p 62.

43. Budzikiewicz, H.; Djerassi, C.; Williams, D. H. *Mass Spectrometry of Organic Compounds*; Holden-Day: San Francisco, 1967; Chap. 6, Sec. 6.3, pp. 258–268.